SOCAR Proceedings

*Reservoir and Petroleum Engineering*

journal home page: http://proceedings.socar.az

# THE INFLUENCE OF PORE STRUCTURE ON WATER FLOW IN ROCKS FROM THE BEIBU GULF OIL FIELD IN CHINA

**R.Shen[1,2]*, X.Lei[3], H.K.Guo[1,2], H.T.Zhou[1,2], Q.Zhang[4], H.B.Li[1,2]**

[1]*Department of Porous Flow & Fluid Mechanics, PetroChina RIPED, Langfang, China;*
[2]*Key Laboratory of Petrophysics and Fluid Flow through Porous Media, CNPC, Langfang, China;*
[3]*Zhanjiang Branch of China National Offshore Oil Corporation, CNOOC, Zhangjiang, China;*
[4]*Energy Technology & Service-oilfield Engineering Research Institute, CNOOC, Zhanjiang, China*

***A b s t r a c t***

Large differences in water flooding efficiency of patterns in different blocks of the Beibu Gulf oil field in China, were taken as an example of water flow problems leading to reduced recovery factor. Cores of formation $W_3$IV in Well W and formation $L_3$III in Well B were taken for study. By combining dynamic nuclear magnetic resonance, constant-rate mercury injection and a visual micro plate model, the flow characteristics and factors influencing the pore scale flow of water were analyzed for these reservoirs. The pore and throat radii were small, but the pore throat ratio is large and its distribution range was wide. So, for example the pore volume of Well B samples was mainly controlled by smaller throats. It is easy for a dominant injection water flow path to form under such conditions and this adversely affects the volumetric sweep efficiency of the water flooding. The mechanism of this is explained. It results in oil recovery in medium and small pores of up to about 40%, while that in large pores is less than 5%. As a consequence the average oil displacement efficiency of Well B was only 44.7%, which is 22.3% lower than that of Well W.

***Keywords:***
Nuclear magnetic resonance;
Water flooding;
Oil displacement efficiency;
Sweep efficiency;
Pore throat structure.



## Introduction

For high-efficiency development of water flooding reservoirs in their middle and late stages, it is fundamental and critical to investigate and recognize the factors affecting injected water sweep in pores with different sizes. Nuclear magnetic resonance (NMR) core analysis can be used to detect the NMR signal intensity and the $T_2$ relaxation time of the hydrogen atoms in the pore fluids in samples. The NMR signal intensity reflects total fluid volume in pores. The $T_2$ relaxation time reflects the force acting on the fluid affected by the rock pore surfaces, indirectly corresponding to pore size [1-10]. In core tests to analyze the microscopic mechanism of oil and water two-phase flow in pores with of different sizes, dehydrogenated kerosene is used to eliminate NMR signal of oil [11], then the distribution of water-bearing pore sizes and water saturation in the pores are determined. By combining pore-throat distribution features, and visualized microscopic flow simulation results, the influences of pore-throat type, structure and distribution features on water flooding were comprehensively analyzed, to provide a point of reference for an adjusted development strategy of production at moderate to high water content.

## 2. Samples and experimental methods

### *2.1. Sample features*

Core samples were taken from the $W_3$IV layer in Well W in the WZ11-1 block and the $L_3$III layer in Well B in the WZ12-1 block in the Beibu gulf area. The cores from Well W have average gas permeability of 117 mD and average porosity of 19.5%, and the cores from Well B have average gas log permeability of 87 mD and average porosity of 18%. Both wells have similar porosity and permeability values, but Well B has stronger correlation in exponential function relation between porosity and permeability (fig.1). Four cores were selected respectively from the two wells for dynamic NMR water-flooding experiments. The physical properties of these cores are shown in table 1.

**E-mail:* shenrui523@126.com
http://dx.doi.org/10.5510/OGP20170300321

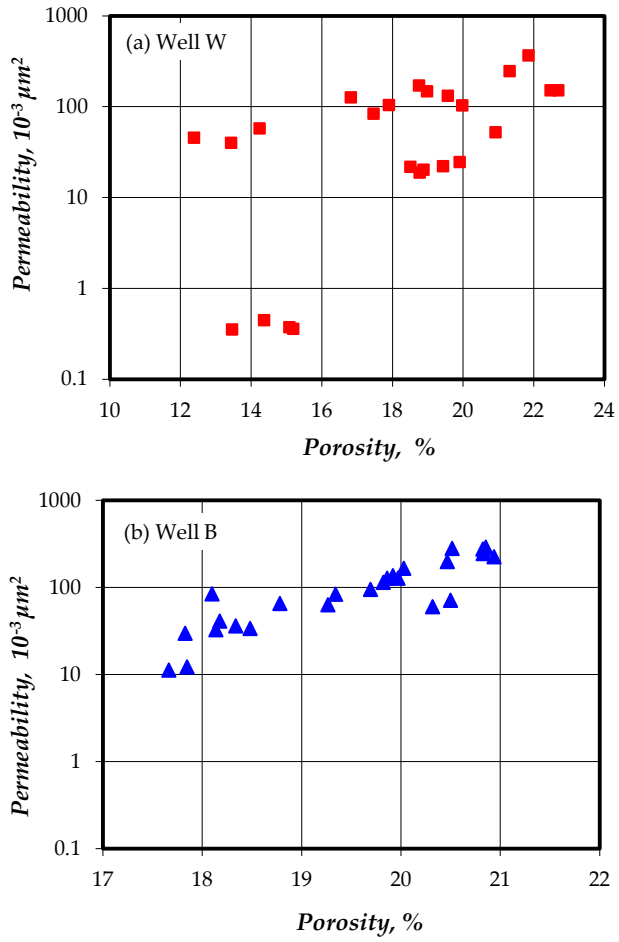


**Fig.1. Relations between porosity and permeability of the cores**

### 2.2. Experimental methods

*2.2.1. Volume-controlled (constant rate) mercury porosimetry*

In volume-controlled porosimetry, mercury is injected at very slow and constant rate into an evacuated sample, so this method is also called constant-rate mercury injection porosimetry. The deepest and shallowest samples of the four cores in each well were selected, so samples B1 and B2 from Well B and samples W1 and W2 from Well W were dried ready for use. About 0.5 cm long regular cores were cut from the middle section of the field cores for testing with the ASPE-730 mercury injection apparatus made by American Coretest Systems, Inc. During the testing, the mercury injection rate was maintained at $1\times10^{-4}$ ml/min, and the maximum mercury injection pressure was 6.12 MPa, corresponding to a lower limit of pore throat radius of about 0.12 μm.

*2.2.2. Water-flooding dynamic NMR experiments*

In current conventional NMR water flooding experiments, the water flooding and NMR testing are conducted separately. When a certain pore volume (PV) has been displaced in the water flooding experiment, the samples are taken out from the core holder then NMR testing is conducted. Because of the change of stress field on the cores, the oil and water distribution in the cores change, thus the $T_2$ spectrum cannot reflect reality. In this study, the water flooding experiments were completed with the RecCore3002 HTHP NMR on-line detection system made by Institute of Porous Flow and Fluid Mechanics, Chinese Academy of Sciences. This system, with the highest confining pressure of 50 MPa, replaces the conventional process and it also eliminates the weakness of the traditional NMR method which cannot be conducted under pressure. Through these experiments, $T_2$ spectra can be obtained at saturated formation water, oil-saturated irreducible water, different degrees of displacement and at water flooding end-point in cores.

The dehydrogenated kerosene used in the experiments is fluorinated and doesn't contain hydrogen, so the oil phase doesn't generate a signal during NMR testing. Thus the measured $T_2$ spectra in various conditions are all $T_2$ spectra of the water phase. The $T_2$ relaxation time reflects the size of pores, and the envelope area increment of the spectrum in different states indicates the recovery degree of water flooding. By analyzing the $T_2$ spectrum changes, the oil content and the oil phase distribution in the pores of the core at irreducible water saturation were quantified, and the total recovery percentage of oil phase and the recovered percentage of oil phase in different pore sizes at the final water flooding status were quantitatively analyzed.

The experiments were carried out at room tempera-ture to simulate the oil/water viscosity ratio in the reservoir, using the methods specified

**Table 1**

**Property and information of samples**

| Well No. | Sample No. | Depth | Horizon | Porosity, % | Gas permeability, $10^{-3}$ μm² | Water permeability, $10^{-3}$ μm² |
|---|---|---|---|---|---|---|
| B | B1 | 2742 | $W_3$IV | 21.22 | 70.66 | 20.33 |
| B | B2 | 2748.53 | $W_3$IV | 20.76 | 259.17 | 20.75 |
| B | B3 | 2744.3 | $W_3$IV | 20.37 | 88.25 | 19.57 |
| B | B4 | 2745.72 | $W_3$IV | 18.76 | 30.35 | 18.21 |
| W | W1 | 2699.76 | $L_3$III | 14.33 | 64.66 | 13.37 |
| W | W2 | 2665.82 | $L_3$III | 22.09 | 46.66 | 20.19 |
| W | W3 | 2698.09 | $L_3$III | 18.47 | 92.09 | 17.33 |
| W | W4 | 2682 | $L_3$III | 15.71 | 56.8 | 13.69 |

in China's oil and gas industry standards: «Method of core analysis (SY/T5336-2006)» and «The method for measuring relatively permeability in two-phase fluid in rocks (SY/T5345-2007)».

## 3. Pore-throat structure features

### *3.1. Mercury injection features in constant-rate mercury injection experiment*

Constant-rate mercury injection experiments can record three curves; mercury injection in pores, mercury injection in throats, and total mercury injection. For samples from Well B, as the pressure increases, the total mercury injection curve always coincides with the mercury injection in throats. Moreover, the mercury injection in throats always increases, but the incremental mercury injection in pores only corresponds to a narrower pressure range (fig.2a). This means that samples of Well B have fewer pores being controlled by throats [12-16]. However, the mercury injection characteristics of the well W samples were different with uptake being controlled by pore bodies during early mercury injection, then as pressure increased the total mercury injection was controlled by pore throats (fig.2b).

### *3.2. Distribution features of pore-throats*

Figure 3 shows the distribution curves of pore radius, throat radius and pore/throat ratio that were obtained by constant-rate mercury injection. The pore throats only reflect the parts connecting the pores. The pores and throats of samples B1 and B2 are relative uniform. The major throat radii are 1-6 μm (with peak of 2-4 μm); the major pore radii are 90-200 μm (with peak of about 130 μm). The pore/throat ratios are 20-100. Sample W1 has major throat radii of 11-12 μm, pore radii of 200-400 μm, and peak of 300 μm. Sample W2 has major throat radii of 6-8 μm, pore radii of 120-300 μm, and peak of 180 μm. The peak pore/throat ratios of the two samples are both around 25. Apparently, samples from Well W have bigger pore radii and throat radii, and smaller

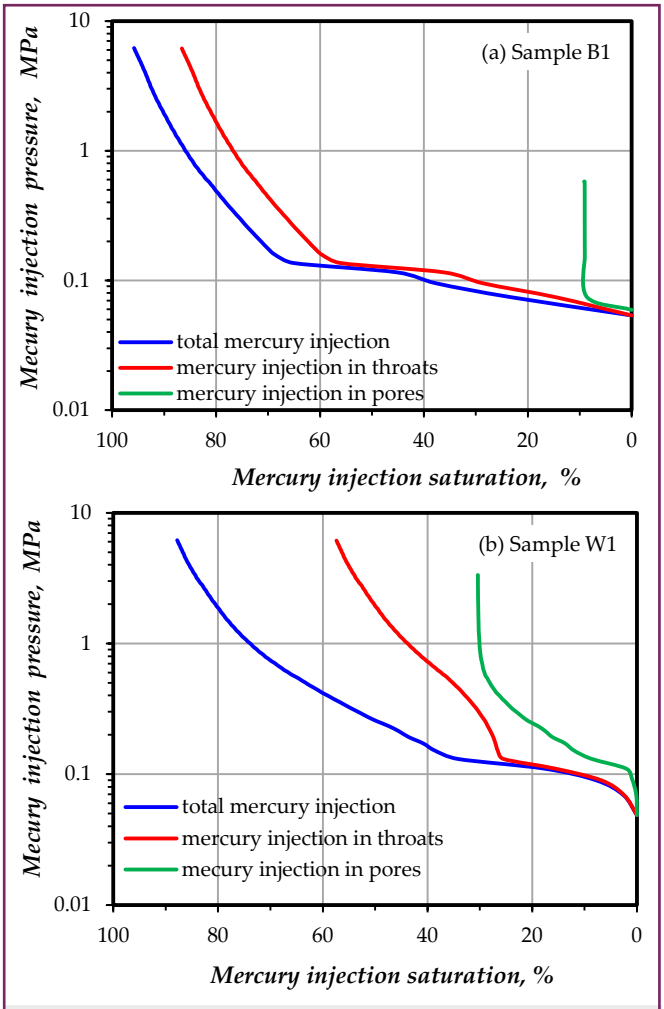


**Fig.2. Constant-rate mercury injection curves of typical samples**

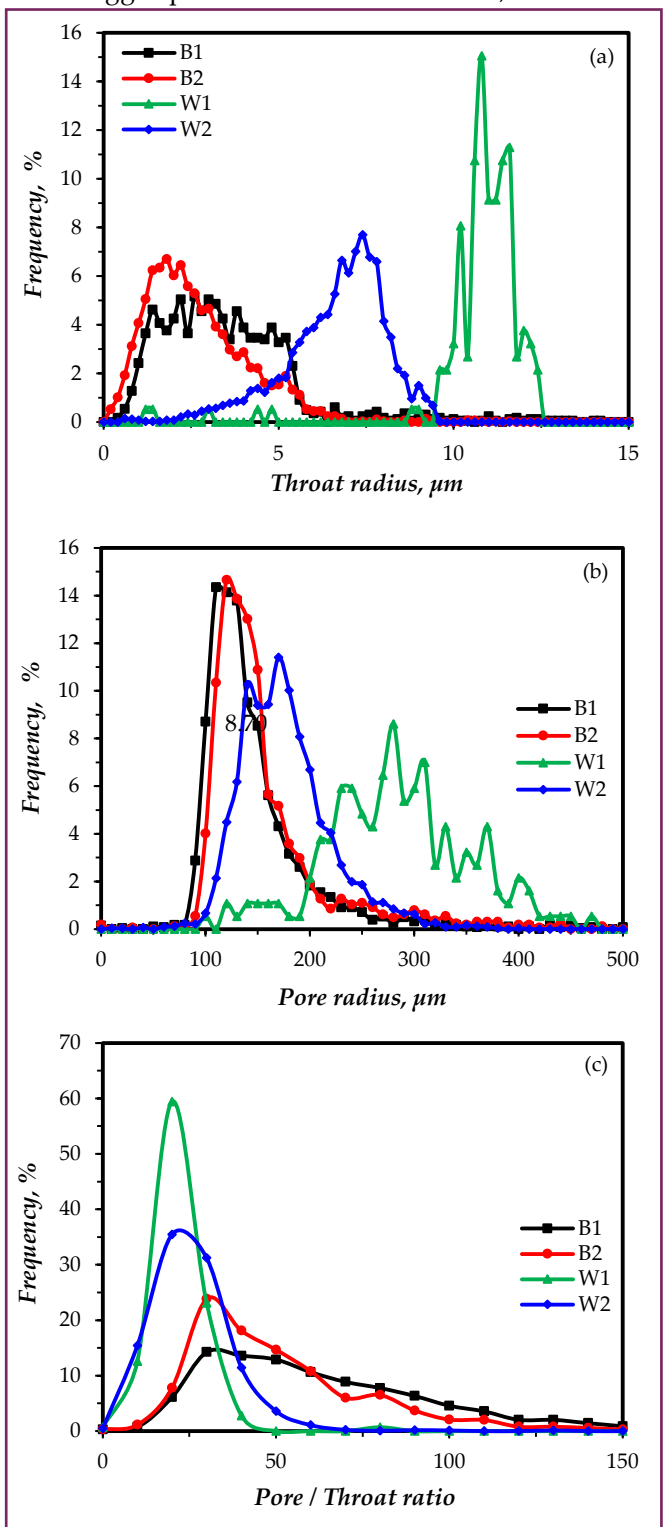


**Fig.3. Distribution curves of pore radius, throat radius and pore/throat ratio**

pore/throat ratios. Compared with the samples from Well W, the samples from Well B have bigger and more widely-distributed pores and throats; the single pores are controlled by small throats. When water flooding, oil flows through small throats, and there is bigger resistance; once the injected water breaks through in some pore throats, predominant flow pathways are more easily formed. The smaller pore throats have huge capillary resistance, thus the injected water can hardly sweep them.

## 4. Results of water flooding dynamic NMR experiment and discussion

### *4.1. NMR $T_2$ spectra*

Figure 4 shows the NMR $T_2$ spectra of cores in four states: saturated with formation water, at oil-saturated irreducible water (initial oil saturation), different displacing quantity status, and final water flooding saturation (residual oil saturation). The relaxation time of NMR $T_2$ reflects pore sizes, and it has positive relation with pore radius. Using the NMR $T_2$ relaxation time, the pores can be divided into middle-small pores (<100 ms) and big pores (>100 ms). Hence, the NMR experiment can be used to get the oil content in all pores of the cores, and to quantitatively analyze the oil content in pores of different sizes and recovery states.

### *4.2. Oil content in pores with different sizes and recovery status*

Table 2 shows the water flooding NMR test results of eight samples. The initial oil saturation of all the cores is similar (averaging 55.57% and 55.33% in cores from the two wells, respectively). The average recovery ($R_e$) of the samples from Well W was 22.34% higher than that from Well B.

For four samples from Well B, the average absolute oil saturation in big pores was 20.3%, that in medium to small pores was 35.3%, and the oil quantity in medium to small pores was 15% higher than that in big pores. For four samples from Well W, the average absolute oil saturation in big pores was up to 40.9%, that in medium to small pores was 14.4%, and the oil quantity in big pores was 26.5% higher than that in medium to small pores.

At residual oil saturation ($S_{or}$) the average water flooding recovery of the samples from Well B was 44.7%, which is lower than that from Well

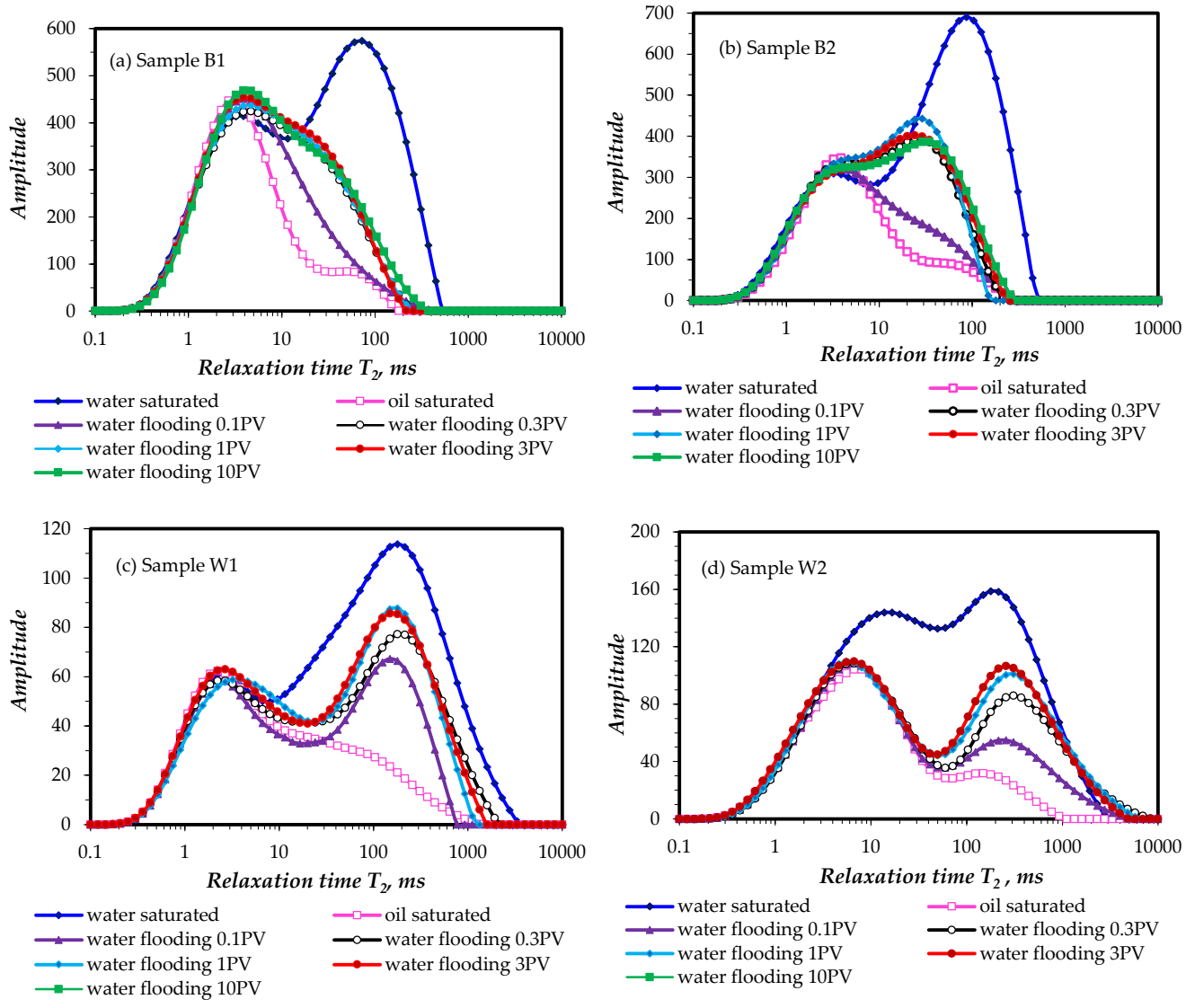


**Fig.4. NMR $T_2$ spectra of core samples in various states**

Table 2

NMR results in irreducible water and residual oil conditions

| Sample No. | $S_{or}$, % | | | $R_e$, % | | |
|---|---|---|---|---|---|---|
| | Middle-small pores | Big pores | All pores | Middle-small pores | Big pores | All pores |
| B1 | 33.36 | 20.56 | 53.92 | 37.87 | 5.62 | 43.5 |
| B2 | 34.51 | 25.56 | 60.07 | 37.77 | 5.26 | 43.03 |
| B3 | 33.47 | 17.22 | 50.69 | 43.25 | 4.45 | 47.7 |
| B4 | 39.9 | 17.69 | 57.59 | 40.97 | 3.66 | 44.62 |
| W1 | 16.88 | 37.56 | 54.44 | 14.34 | 51.67 | 66.02 |
| W2 | 24.91 | 32.74 | 57.65 | 14.5 | 49.95 | 64.46 |
| W3 | 6.52 | 48.95 | 55.47 | 2.26 | 65.85 | 68.11 |
| W4 | 9.48 | 44.26 | 53.74 | 14.66 | 54.95 | 69.61 |

W. The average recovery degree in large pores was only 4.8%, which is much lower than that from Well W (55.6%).

## 5. The influences of pore type and structure on water flooding

### *5.1. Pore-throat distribution*

*5.1.1. A brief introduction to the microscopic visualization model*

The microscopic simulation glass model is a transparent two-dimensional glass model developed by Department of Porous Flow and & Fluid Mechanics, Research Institute of Petroleum Exploration and & Development, PetroChina Company Limited. The real pore system of a core slice is extracted by a photochemical etching process, precisely etched onto flat glass, and finally sintered at high temperature. The microscopic model of water flooding experiment is placed under vacuum then fully saturated by water, fully saturated by crude oil, and then attached to the micro model holder. Water flooding tests were carried out at recorded temperatures, pressures and velocities. The experimental microscopic model was placed under a microscope, and the process of water flooding was recorded by digital cameras.

The pore-throats of the samples from Well B have bigger and more widely-distributed pore-throat ratio (fig.5). Single pores are controlled by small throats. When water flooding, oil flows through small throats, and there is bigger resistance; once the injected water breaks through in some throats, it will displace oil in these pores and predominant water flow pathways are formed, which can influence the swept volume of the model (fig.6).

The samples from Well W have larger pore radii and throat radii, smaller and narrowly-distributed

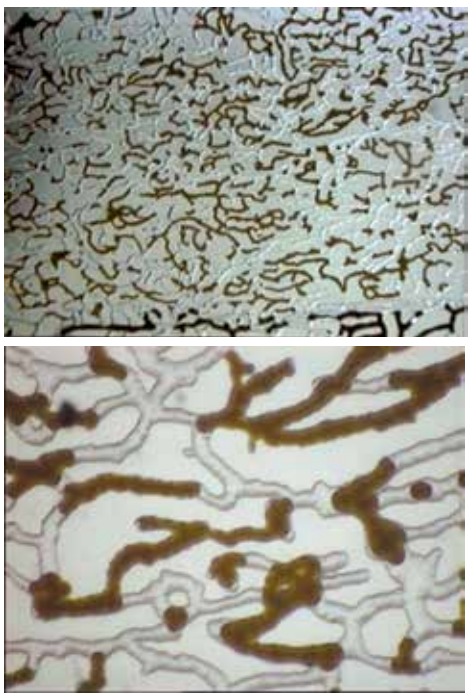


Fig.5. Oil and water distribution at residual oil saturation for the microscopic visualized model of samples from Well B: a) Full view; b) Local zoom-in

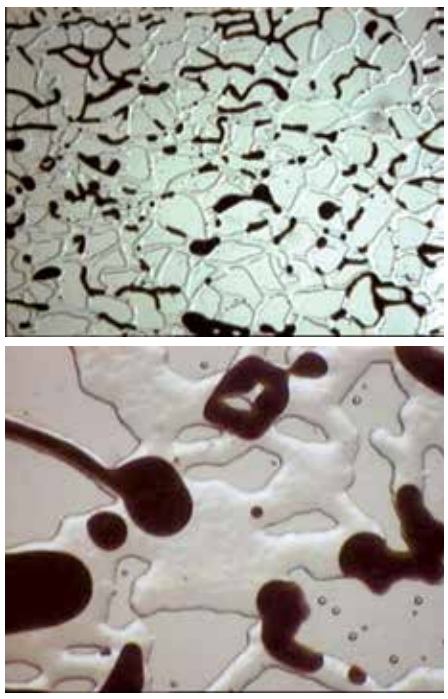


Fig.6. Oil and water distribution at residual oil saturation for the microscopic visualized model of samples from Well W: a) Full view; b) Local zoom-in

pore/throat ratios, small pore volume/throat volumes. Single pores are controlled by multiple bigger throats. The oil in the pores easily flows through throats and is displaced by the injected water. The injected water has relatively uniform swept areas, higher sweep efficiency, and more oil in pores can be displaced (fig.6).

In summary, the samples from Well B have smaller throat radii, bigger pore/throat ratio, wider distribution. Thus some oil in pores of Well B has not been swept by the injected water, which affects the final crude oil recovery degree. So, the oil recovery form the well B cores was lower than those from the Well W.

## Conclusions

1. The combination of constant-rate mercury injection and water flooding dynamic NMR experiments can help to quantitatively evaluate the features of oil occurrence and recovery status in pores with different sizes, and to confirm the influences of pore-throat types and structures on oil producing law in such pores.

2. Pore-throat structures are major factors leading to differences in water flood performance in the Beibu-gulf area rock samples studied. The samples from Well B have smaller pore-throats, bigger pore/throat ratio, and wider distribution; single pores are controlled by small throats. When the oil flows through small pore throats, it is more difficult to recover.

*This research was supported by the National Science and Technology Major Project of China(Grant No.2017ZX05037001) and the Project of Southwest Oil and Gas Fields PetroChina(2016E-0611).*

***Reference***

1. *Y.Zhang, C.Y.Song, D.Y.Yang.* A damped iterative EnKF method to estimate relative permeability and capillary pressure for tight formations from displacement experiments //Fuel. –2016. –Vol.167. –P.306-315.

2. *K.Katika, M.Addassi, M.M.Alam, et al.* The effect of divalent ions on the elasticity and pore collapse of chalk evaluated from compressional wave velocity and low-field Nuclear Magnetic Resonance (NMR) //Journal of Petroleum Science and Engineering. –2015. –Vol.136. –P.88-99.

3. *L.L.Barbosa, F.V.C.Kock, V.M.D.L.Aleida, et al.* Low-field nuclear magnetic resonance for petroleum distillate characterization //Fuel Processing Technology. –2015. –Vol.138. –P.202-209.

4. *H.Gao, H.Z.Li.* Determination of movable fluid percentage and movable fluid porosity in ultra-low permeability sandstone using nuclear magnetic resonance (NMR) technique //Journal of Petroleum Science and Engineering. –2015. –Vol.133. –P.258-267.

5. *Y.B.Yao, D.M.Liu.* Comparison of low-field NMR and mercury intrusion porosimetry in characterizing pore size distributions of coals //Fuel. –2012. –Vol.95. –P.152-158.

6. *O.Talabi, M.J.Blunt.* Pore-scale network simulation of NMR response in two-phase flow //Journal of Petroleum Science and Engineering. –2010. –Vol.72. –P.1-9.

7. *Y.Q.Song*. Novel NMR techniques for porous media research //Cement and Concrete Research. –2007. –Vol. 37. –No.3. –P.325-328.

8. *S.H.Al-Mahrooqi, C.A.Grattoni, A.K.Moss, et al.* An investigation of the effect of wettability on NMR characteristics of sandstone rock and fluid systems //Journal of Petroleum Science and Engineering. –2003. –Vol.39. –No3. –P389-398.

9. *A.T.Watson, C.T.P.Chang.* Characterizing porous media with NMR methods //Progress in Nuclear Magnetic Resonance Spectro. –1997. –Vol.31. –P.344-383.

10. *R.L.Kleinberg.* Utility of NMR $T_2$ distributions, connection with parameter pz pressure, clay effect, and determination the surface relaxivity parameter $\varrho_2$ //Magnetic Resonance Imaging. –1996. –Vol.14. –No.7. –P.761-767.

11. *M.P.Enwere, J.S.Archer.* Some insight into laboratory core floods using an NMRI technique // Journal of Petroleum Science and Engineering. –1994. –Vol.11. –No.2. –P.73-89.

12. *R.R.Sharipov, A.A.Coyedjo, J.M.Quagu, et al.* Development of reagents for enhanced oil recovery of high-temperature formations//SOCAR Proceedings. –2017. –No.2. –P.62-67.

13. *A.Nepryahin, E.M.Holt, R.S.Fletcher, et al.* Structure-transport relationships in disordered solids using integrated rate of gas sorption and mercury porosimetry //Chemical Engineering Science. –2016. –Vol.152. –P.663-673.

14. *D.Pastorino, C.Canal, M.Ginebra.* Multiple characterization study on porosity and pore structure of calcium phosphate cements //Acta Biomaterialia. –2015. –Vol.28. –P.205-214.

15. *A.A.Efimov, Y.V.Savitskiy, S.V.Galkin, et al.* Study of wettability of reservoirs of oil fields by the method of x-ray tomography core //SOCAR Proceedings. –2016. –No.4. –P.55-63.

16. *F.Zhao, R.Shen, S.S.Gao, et al.* Application and calculation method of waterflood front in low permeability reservoir //Journal of the Japan Petroleum Institute. –2014. –Vol.57. –No.6. –P.271-275.

# Влияние поровой структуры на движение воды в породах нефтяного месторождения в заливе Бэйбу (Китай)

***Р.Шен[1,2], К.Лей[3], Х.К.Гуо[1,2], Х.Т.Жу[1,2], Г.Жанг[4], Х.Б.Ли[1,2]***
[1]Департамент механики жидкости в пористой среде, PetroChina RIPED, Ланфан, Китай; [2]Лаборатория петрофизики и потока жидкости через пористую среду, CNPC, Ланфан, Китай; [3]Чжаньцзянский филиал Китайской национальной шельфовой нефтяной корпорации (CNOOC), Чжанцзян, Китай; [4]НИИ нефтегазосервисного инжиниринга и энергетических технологий, CNOOC, Чжанцзян, Китай

## Реферат

Статья посвящена проблемам, связанным с продвижением воды в пласте, приводящих к снижению коэффициента извлечения. Представлен анализ эффективности процесса заводнения на различных блоках нефтяного месторождения в заливе Бэйбу (Китай). Для исследований использовались образцы керна из пласта $W_3$IV в скважине W и пласта $L_3$III в скважине B. Используя методы динамического ядерного магнитного резонанса, ртутной порометрии с постоянным расходом и модель микропланшетной визуализации, были проанализированы реологические свойства пластовой жидкости и факторы, влияющие на её продвижение в рассматриваемых пластах. Исследуемая среда характеризуется невысокими значениями радиусов пор и поровых каналов, высокими значениями коэффициента сообщаемости пор и его диапазона распределения. Поровое пространство в образцах керна, взятых из скважины B имело меньшую сообщаемость. Очевидно, что основной поток закачиваемой жидкости формируется под влиянием пластовых условий. Это может отрицательно сказываться на вытесняющей способности воды. Приводится механизм этого процесса. В результате извлечение нефти из пор среднего и малого размера составляет около 40%, тогда как в порах большего размера - менее 5% порового объема. Как следствие, средний коэффициент нефтевытеснения из пласта вокруг скважины B составлял всего 44.7%, что на 22.3% ниже, чем у скважины W.

***Ключевые слова:*** ядерный магнитный резонанс; заводнение; коэффициент нефтевытеснения; коэффициент охвата вытеснением; структура поровых каналов.

# Beybu (Çin) körfəzində neft yatağının süxurlarında suyun hərəkətinə məsaməli strukturun təsiri

***R.Şen[1,2], K.Ley[3], X.K.Quo[1,2], X.T.Ju[1,2], Q.Janq[4], X.B.Li[1,2]***
[1]Məsaməli mühitdə mayenin mexanikası departamenti, PetroChina RIPED, Lanfan, Çin;
[2]Petrofizika və məsaməli mühitdən maye axını laboratoriyası, CNPC, Lanfan, Çin;
[3]Çin milli neft şelf korporasiyasının (CNOOC) Çjanszyan filialı, Çjanszyan, Çin;
[4]Neftqazservis mühəndisliyi və energetika texnologiyaları ETİ, CNOOC, Çjanszyan, Çin

## Xülasə

Məqalə hasilat əmsalının azalmasına səbəb olan, layda suyun hərəkəti ilə bağlı problemlərə həsr edilmişdir. Beybu (Çin) körfəzində neft yatağının müxtəlif bloklarında suvurma prosesinin səmərəliliyinin təhlili verilmişdir. Tədqiqatlar üçün W quyusunda $W_3$IV layından və B quyusunda $L_3$III layından götürülmüş kern nümunələri istifadə olunmuşdur. Dinamik nüvə maqnit rezonansı, sabit sərfli civə porometriyası üsullarından və mikroplanşetli vizuallaşdırma modelindən istifadə edərək, lay mayesinin reoloji xassələri və baxılan laylarda onun hərəkətinə təsir edən amillər təhlil edilmişdir. Tədqiq edilən mühit məsamələrin və məsamə kanallarının radiuslarının kiçik qiymətləri, məsamələrin qarşılıqlı əlaqə əmsalının və onun paylanma diapazonunun yüksək qiymətləri ilə xarakterizə olunur. B quyusundan götürülmüş kern nümunələrində məsaməli mühitin qarşılıqlı əlaqəsi kiçik olmuşdur. Təbiidir ki, vurulan mayenin əsas axını lay şəraitinin təsiri altında formalaşır. Bu, suyun sıxışdırma qabiliyyətinə mənfi təsir göstərə bilər. Məqalədə bu prosesin mexanizmi verilir. Nəticədə orta və kiçik ölçülü məsamələrdən neftin çıxarılması məsamə həcminin təxminən 40%-ni təşkil etmişdir, halbuki böyük ölçülü məsamələrdən neftin çıxarılması məsamə həcminin 5%-dən az olmuşdur. Beləliklə, B quyusu ətrafında laydan orta neftsıxışdırma əmsalı cəmi 44.7% təşkil edir ki, bu W quyusuna nisbətən 22.3% aşağıdır.

***Açar sözlər:*** nüvə maqnit rezonansı; suvurma; neftsıxışdırma əmsalı; sıxışdırmanın əhatə əmsalı; məsamə kanallarının strukturu.